IOPscience iopscience.iop.org

Home Search Collections Journals About Contact us My IOPscience

Critical phase transition temperatures of 1–3 type multiferroic composite thin films

This content has been downloaded from IOPscience. Please scroll down to see the full text.

2007 J. Phys. D: Appl. Phys. 40 1614

(http://iopscience.iop.org/0022-3727/40/6/004)

View the table of contents for this issue, or go to the journal homepage for more

Download details:

IP Address: 113.108.133.53
This content was downloaded on 18/07/2017 at 09:22

Please note that terms and conditions apply.

You may also be interested in:

Phenomenological theory of 1–3 type multiferroic composite thin film
XiaoYan Lu, Biao Wang, Yue Zheng et al.

Surface tension and size effect in ferroelectric nanotubes
Yue Zheng, C H Woo and Biao Wang

A novel nanostructure and multiferroic properties in Pb(Zr0.52Ti0.48)O3/CoFe2O4 nanocomposite films
J X Zhang, J Y Dai, W Lu et al.

Adjustable ferroelectric properties in paraelectric/ferroelectric/paraelectric trilayers
XiaoYan Lu, Biao Wang, Yue Zheng et al.

Bending response of terfenol-D/BaTiO3 bilayer to external magnetic and electric fields
XiaoYan Lu, Biao Wang, Yue Zheng et al.

Theory of magnetoelectric coupling in 2–2-type magnetostrictive/piezoelectric composite film with texture
Chao-Qian Liu, Wei-Dong Fei and Wei-Li Li

The single-phase multiferroic oxides: from bulk to thin film
W Prellier, M P Singh and P Murugavel

Coupling interaction in multiferroic BaTiO3–CoFe2O4 nanostructures
Gang Liu, Ce-Wen Nan, Z K Xu et al.

Multifunctional magnetoelectric materials for device applications
N Ortega, Ashok Kumar, J F Scott et al.

IOP PUBLISHING JOURNAL OF PHYSICS D: APPLIED PHYSICS

J. Phys. D: Appl. Phys. **40** (2007) 1614–1619 doi:10.1088/0022-3727/40/6/004

Critical phase transition temperatures of 1–3 type multiferroic composite thin films

XiaoYan Lu[1], Biao Wang[1,3], Yue Zheng[1] and Earle Ryba[2]

[1] Electro-Optics Technology Center, Harbin Institute of Technology, Harbin 150001, People's Republic of China
[2] Department of Materials Science and Engineering, The Pennsylvania State University, University Park, Pennsylvania 16802, USA

E-mail: wangbiao@mail.sysu.edu.cn

Received 21 September 2006, in final form 3 January 2007
Published 2 March 2007

Abstract
The critical phase transition temperatures of the ferroelectric (FE) phase and the ferromagnetic (FM) phase in epitaxial 1–3 type multiferroic thin films were obtained based on the thermodynamic model. Analytic expressions of the para–ferro transition temperatures were derived as functions of the volume fraction of the FM phase by considering the effect of the coupled elastic stresses arising from the FE/FM and the film/substrate interfaces. Our results show that the critical temperatures are significantly affected by the induced stresses and can be controlled by adjusting the volume fractions of the different phases within the thin film.

(Some figures in this article are in colour only in the electronic version)

1. Introduction

Multiferroic materials with two or three coupled ferroelectric (FE), antiferromagnetic/ferromagnetic (FM) and ferroelastic properties are currently being intensively investigated because of their potential applications in the emerging field of spintronics, new data-storage media [1], multiple-state memories and sensors [2]. However, materials with large magneto-electric (ME) coupling rarely exist in nature because transition-metal *d* electrons reduce the tendency for non-centric ferroelectric distortion [2]. Over the past few years, advances in nanoscale thin films and characterization techniques have led to the development of excellent structures with good performance, revealing rich and fascinating phenomena.

The ME coupling effect, which uses magnetic fields to control electric properties, and vice versa, is of fundamental and technological interest and has led to the renaissance of multiferroic materials. Recently, studies have focused on Bi-based compounds, including those with Bi site substitutions (e.g. $BiMnO_3$ [3], $BiFeO_3$ [4], Bi_2FeCrO_6 and $BiCrO_3$ [5]), rare earth (RE) manganites ($REMnO_3$ [6] and $REMn_2O_5$ [7]), and composite materials with two or three phases [8–10], following the ideas of van Schtelen [11]. Large ME coupling responses [12, 13] at room temperature have been found, but a comprehensive understanding of the coupling mechanism is lacking, especially for single phase multiferroic materials.

It is widely believed that ME coupling arises from the interaction of internal and external stresses in composite thin films. The effects of strain are regarded to be significant or even dominant [14] and relate to factors such as the lattice parameters of each phase and the substrate, magnetostrictive and electrostrictive properties and the volume fractions of each part. Such factors must be well understood to develop materials with large ME effects. Theoretical approaches, including the Green's function technique [15], and phenomenological models using the Landau–Ginzburg–Devonshire theory [16] have been used to describe FE and FM coupling. However, the details of the effect of external/internal stress on the properties of the 1–3 type (three-dimensional heteroepitaxy structure [9, 17]) multiferroic thin films have not been investigated. This paper presents the results of an investigation of the effects of stress on the critical temperatures which govern the time-dependent Ginzburg–Landau (TDGL) equations for the evolutions of both the polarization and the magnetization.

---

[3] Author to whom any correspondence should be addressed. Also at: The State Key Lab of Optoelectronic Materials and Technologies, School of Physics and Engineering, Sun Yat-sen University, Guangzhou, People's Republic of China.

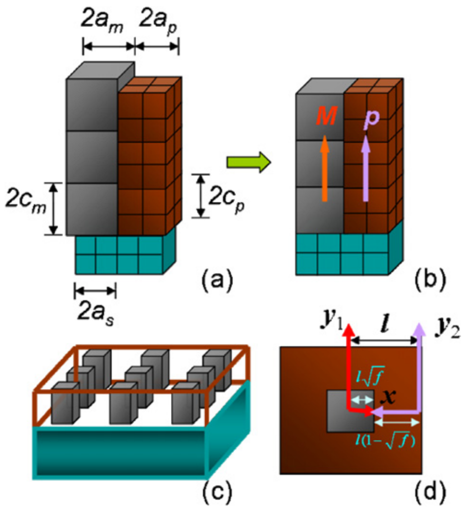

Figure 1. Schematic of the calculation model. (*a*) Schematic illustration of the free standing states of each part, (*b*) the state after transmutation with lattices well matched, (*c*) heterostructure of the 1–3 type with the FM phase (in grey) imbedded in the FE phase (in crimson) on a rigid substrate (in blue), and (*d*) the cross section of one element, in which *l* is half of the element length. (Colour online.)

2. Thermodynamic model and stability of the stationary state

A 1–3 type $BaTiO_3$–$CoFe_2O_4$ thin film grown on a $SrTiO_3$ substrate was studied based on the experiments [9, 17]. The model used is defined in figure 1. Two local coordinate systems with x, y and z parallel to the [1 0 0], [0 1 0] and [0 0 1] directions, respectively, in the crystals were chosen for the FE and FM phases (figure 1(*d*)). It was assumed that the magnetic component is perpendicular to the interface of the film/substrate since the easy magnetic axis is along the [0 0 1], and in the same direction as the FE polarization in tetragonal $BaTiO_3$. Since the properties of the material are the same along the x and y axes, the order parameters can be simplified to functions of x and z. The depolarization field may be greater in a thin film but weaker in a cylinder. In this work, the depolarization effect was ignored for simplicity. The total free energy of the system with order parameters P for the FE phase and M for the FM phase is [16, 18]

$$F = F_l^E + F_l^M + F_{\mathrm{elas}} + F_{\mathrm{surf}}, \tag{1}$$

where F_l^E and F_l^M are the Landau type bulk free energies of the FE and FM phases, respectively, F_{elas} is the elastic energy of the total body and F_{surf} is the surface energy describing the relaxation of the surface lattices and the relaxation or restriction of the interfacial lattice. F_l^E, F_l^M and F_{surf} can be expressed as

$$F_l^E = (1-f)\int_v \left[\frac{A^E}{2}(T-T_{c0}^E)P^2 + \frac{B^E}{4}P^4 + \frac{C^E}{6}P^6 + \frac{D_{44}^E}{2}\left(\frac{\partial P}{\partial x}\right)^2 + \frac{D_{11}^E}{2}\left(\frac{\partial P}{\partial z}\right)\right]\mathrm{d}v, \tag{2}$$

$$F_l^M = f\int_v \left[\frac{A^M}{2}(T-T_{c0}^M)M^2 + \frac{B^M}{4}M^4 + \frac{D_{44}^M}{2}\left(\frac{\partial M}{\partial x}\right)^2 + \frac{D_{11}^M}{2}\left(\frac{\partial M}{\partial z}\right)^2\right]\mathrm{d}v, \tag{3}$$

$$F_{\mathrm{surf}} = (1-f)\int_s \frac{P^2}{2\delta_{p_z}}\mathrm{d}s + f\int_s \frac{M^2}{2\delta_{m_z}}\mathrm{d}s + \int_{s_i}\left(\frac{P^2}{2\delta_{p_x}} + \frac{M^2}{2\delta_{m_x}}\right)\mathrm{d}x, \tag{4}$$

where A^E, B^E, C^E, D_{44}^E, D_{11}^E and T_{c0}^E are the Landau type expansion coefficients for the bulk free energy and the Curie temperature, respectively, of the FE phase.

A^M, B^M, D_{44}^M, D_{11}^M and T_{c0}^M are the Landau type expansion coefficients for the bulk free energy and the Curie temperature, respectively, of the FM phase. f is the volume fraction of the FM phase. v and s are the volume and the surface area of the element, respectively. s_i is the interface area of the two phases. δ_{p_x}, δ_{p_z} and δ_{m_x}, δ_{m_z} are the extrapolation lengths along the x and z axes for the FE and FM phases, respectively. While the interface of the phases is in bilayer systems or superlattices complex [19–21]. A simple boundary condition was used here.

For materials free from any other external forces and surface constraints, there will be a self-equilibrated internal stress created by the incompatibility of the eigenstrains [22]. These are spontaneous strains induced by the ferroelectric or ferromagnetic transitions [23]:

$$\varepsilon_{ij}^E = Q_{ijkl}^E P_k P_l, \quad \varepsilon_{ii}^M = \tfrac{3}{2}\lambda_{100}\left(m_i^2 - \tfrac{1}{3}\right),$$

$$\varepsilon_{ij}^M = \tfrac{3}{2}\lambda_{111} m_i m_j \qquad (i \neq j, m = M/M_s),$$

where Q is the electrostrictive coefficient tensor, λ_{100} and λ_{111} are the magnetostrictive coefficients and M_s is the saturation magnetization of the bulk FM material. A 3 × 3 diagonal matrix with all elements of $\frac{3}{2}\lambda_{100}$ is denoted as λ for such a system. Because of the small values of the magnetostrictive coefficients, the corresponding eigenstrains for the FM phase are usually about two or three orders of magnitude less than the electrostrictive strains, except for some alloys for which the average $\bar{\lambda}$ can be about 2000×10^{-6}. Since the magnetic material will extend or shrink along the direction of the magnetic polarization, depending on the value of λ, the external strain/stress will inhibit or promote the phase transitions. It is very important to predict the conditions appropriate for the design of multiferroic composite materials with large ME coupling.

In our system, the elastic energy can be expressed as

$$F_{\mathrm{elas}} = F_{\mathrm{elas}}^E + F_{\mathrm{elas}}^M,$$
$$F_{\mathrm{elas}}^E = (1-f)\int_v f_{\mathrm{elas}}^E \mathrm{d}v, \; F_{\mathrm{elas}}^M = f\int_v f_{\mathrm{elas}}^M\,\mathrm{d}v, \tag{5}$$

where

$$f_{\mathrm{elas}}^E = \tfrac{1}{2}C_{ijkl}^E e_{kl}^p e_{ij}^p = \tfrac{1}{2}C_{ijkl}^E(\varepsilon_{kl}^p - \varepsilon_{kl}^E)(\varepsilon_{ij}^p - \varepsilon_{ij}^E)$$

and

$$f_{\mathrm{elas}}^M = \tfrac{1}{2}C_{ijkl}^M e_{kl}^m e_{ij}^m = \tfrac{1}{2}C_{ijkl}^M(\varepsilon_{kl}^m - \varepsilon_{kl}^M)(\varepsilon_{ij}^m - \varepsilon_{ij}^M)$$

and are the elastic energy densities with the corresponding elastic strains e_{kl}^p and e_{kl}^m of the FE and FM parts, respectively. C_{ijkl}^E and C_{ijkl}^M are the corresponding elastic moduli. ε_{kl}^p and ε_{kl}^m denote the total strains. ε_{kl}^E and ε_{kl}^M are the eigenstrains of the FE and the FM transformations, respectively. It is assumed that the film was grown epitaxially from a rigid substrate and the lattices matched well. The average strain induced by the substrate as a function of volume fraction can be written as

$$\varepsilon_{11}^{p} = \varepsilon_{22}^{p} = \varepsilon_{11}^{m} = \varepsilon_{22}^{m} = \varepsilon_{11}^{0} = \left(\frac{\sqrt{f}}{a_m} + \frac{1-\sqrt{f}}{a_p} \right) a_s - 1,$$

where a_p, $2a_m$ and a_s are the lattice parameters of the FE, FM and substrate crystals, respectively. Ignoring the distortion in the plane, we can derive $\varepsilon_{12}^{p} = \varepsilon_{21}^{p} = \varepsilon_{12}^{m} = \varepsilon_{21}^{m} = 0$. The other strains ε_{i3}^{p} and ε_{i3}^{m} are derived from the mechanical equilibrium equations for the whole sample body which are the surface free condition $(1-f)\sigma_{33}^{E} + f\sigma_{33}^{M} = 0$ and the displacement consistent condition. The solutions for the FE phase and the FM phase are

$$\varepsilon_{33}^{p} = \frac{-1}{C_{11E}} (2C_{12}^{0}\varepsilon_{11}^{0} - q_{11}^{E}P^2 - f_m)$$

and

$$\varepsilon_{33}^{m} = \frac{-1}{C_{11M}} (2C_{12}^{0}\varepsilon_{11}^{0} - q_{11}^{M}M^2/M_s^2 - f_p)$$

respectively, where

$$C_{12}^{0} = (1-f)C_{12}^{E} + fC_{12}^{M},$$

$$C_{11E} = (1-f)C_{11}^{E} + fC_{11}^{M}\frac{C_p}{C_m},$$

$$C_{11M} = fC_{11}^{M} + (1-f)C_{11}^{E}\frac{C_m}{C_p},$$

$$q_{11}^{E} = (1-f)(2C_{12}^{E}Q_{12} + C_{11}^{E}Q_{11}) + fC_{11}^{M}\frac{C_p}{C_m}Q_{11},$$

$$q_{11}^{M} = f(2C_{12}^{M}\lambda_{12} + C_{11}^{M}\lambda_{11}) + (1-f)C_{11}^{E}\frac{C_m}{C_p}\lambda_{11},$$

$$f_m = f\left[2C_{12}^{M}\lambda_{12}(m^2 - 1/3) + C_{11}^{M}\frac{C_m - C_p}{C_m}\right],$$

$$f_p = (1-f)(2C_{12}^{E}Q_{12}P^2 - C_{11}^{E}\frac{C_m - C_p}{C_p}],$$

f_m is the contribution of the polarization to the magnetization and f_p is the contribution of the magnetization to the polarization. Substituting the above results in equation (5), the elastic energy density functions can be derived.

The temporal evolution of the polarization and the magnetization fields can be described by the TDGL equations [24]:

$$\begin{aligned} \frac{\partial p(x,z,t)}{\partial t} &= -L^E \frac{\partial F}{\partial P(x,z,t)} = -L^E(1-f) \\ &\times \Bigg[A^E(T - T_{c0}^{E})P + B^E P^3 + C^E P^5 \\ &- D_{44}^{E}\frac{\partial^2 P}{\partial x^2} - D_{11}^{E}\frac{\partial^2 P}{\partial z^2} + \partial f_{\mathrm{elas}}^{E}/\partial P \Bigg], \end{aligned} \tag{6}$$

$$\begin{aligned} \frac{\partial M(x,z,t)}{\partial t} &= -L^M \frac{\partial F}{\partial M(x,z,t)} \\ &= -L^M f \Bigg[A^M(T - T_{c0}^{M})M + B^M M^3 - D_{44}^{M}\frac{\partial^2 M}{\partial x^2} \\ &- D_{11}^{M}\frac{\partial^2 M}{\partial z^2} + \partial f_{\mathrm{elas}}^{M}/\partial M \Bigg], \end{aligned} \tag{7}$$

where L^E and L^M are kinetic coefficients related to the domain-wall mobilities, and $A^M = 1/(2\chi T_{c0}^{M})$ and $B^M = 1/(2\chi)$ [25].

The variations on the elastic energy (equation (5)) with respect to the polarization and the magnetization can be derived as the following:

$$\begin{aligned} \partial f_{\mathrm{elas}}^{E}/\partial P &= -2P[(q_{c11} - 2q_{c33}C_{120}/C_{11E})\varepsilon_{11}^{0} \\ &- (q_{cq} - q_{c33}/C_{11E})P^2 - f_m q_{c33}/C_{11E}], \end{aligned} \tag{8}$$

$$\begin{aligned} \partial f_{\mathrm{elas}}^{M}/\partial M &= -2m/M_s\lambda_{11}[(C_{12}^{M} - C_{11}^{M}C_{120}/C_{11M})2\varepsilon_{11}^{0} \\ &- C_{11}^{M}(\lambda_{11} - q_{11}^{M}/C_{11M})(m^2 - \frac{1}{3}) - f_p C_{11}^{M}/C_{11M}], \end{aligned} \tag{9}$$

where

$$\begin{aligned} q_{c11} &= 2Q_{12}(C_{11}^{E} + C_{12}^{E}) + 2Q_{11}C_{12}^{E}), \\ q_{c33} &= 2Q_{12}C_{12}^{E} + Q_{11}C_{11}^{E}, \\ q_{cq} &= Q_{12}[2Q_{12}(C_{11}^{E} + C_{12}^{E}) + 2Q_{11}C_{12}^{E}] \\ &\quad + Q_{11}(2Q_{12}C_{12}^{E} + Q_{11}C_{11}^{E}). \end{aligned}$$

The surface items yield the boundary conditions as

$$\begin{aligned} &\frac{\partial P}{\partial z} = \pm\frac{P}{\delta_{pz}} \ \text{for } z = \pm\frac{h}{2}, \quad \frac{\partial P}{\delta x} = -\frac{P}{\partial_{px}} \ \text{for } x = l_p, \\ &\qquad \frac{\partial P}{\partial n} = 0, \ \text{for } x = 0, \\ &\frac{\partial M}{\partial z} = \pm\frac{M}{\delta_{mz}} \ \text{for } z = \pm\frac{h}{2}, \quad \frac{\partial M}{\delta x} = -\frac{M}{\partial_{px}} \ \text{for } x = l_m, \\ &\qquad \frac{\partial M}{\partial n} = 0, \ \text{for } x = 0, \end{aligned} \tag{10}$$

where $l_p = (1-\sqrt{f})l$ and $l_m = (1-\sqrt{f})l$ with the considering element length of the sample as shown in figure 1(*d*). h is the thickness of the film.

According to linear analysis theory, the dynamic stabilities of the stationary states can be probed by applying infinitesimal perturbations Δ_p and Δ_m to the trivial stationary solutions $P_0 = 0$ and $M_0 = 0$. Neglecting the small higher order terms and retaining only the terms linear in Δ_p and Δ_m, equations (6) and (7) become

$$\frac{\partial \Delta_p}{\partial t} = -L^E(1-f)\left(A^{E'}\Delta_p - D_{11}^{E}\frac{\partial^2\Delta_p}{\partial z^2} - D_{44}^{E}\frac{\partial^2\Delta_p}{\partial x^2} \right), \tag{11}$$

$$\frac{\partial \Delta_m}{\partial t} = -L^M f(A^{M'}\Delta_m - D_{11}^{M}\frac{\partial^2\Delta_m}{\partial z^2} - D_{44}^{M}\frac{\partial^2\Delta_m}{\partial x^2}), \tag{12}$$

where

$$\begin{aligned} A^{E'} &= A^E(T - T_{c0}^{E}) - 2 \\ &\quad \times[(q_{c11} - 2q_{c33}C_{120}/C_{11E})\varepsilon_{11}^{0} - f_m q_{c33}/C_{11E}], \\ A^{M'} &= A^M(T - T_{c0}^{M}) - 2/M_s\lambda_{11}[(C_{12}^{M} - C_{11}^{M}C_{120}/C_{11M})2\varepsilon_{11}^{0} \\ &\quad - C_{11}^{M}f_p/C_{11M} + \tfrac{1}{3}C_{11}^{M}(\lambda_{11} - q_{11}^{M}/C_{11M})]. \end{aligned}$$

In the same way, the boundary conditions (equations (10)) can be derived only with P and M replaced by Δ_p and Δ_m, respectively.

3. Stability analyses of the paraelectric/magnetic states and the critical characteristics

When the sample was cooled below the critical temperatures, a phase transition occurred. The critical conditions can be studied through a bifurcation analysis of the nonlinear equations. As the critical temperatures for the FE phase and the FM phase transitions may be different, a different sequence of transitions will occur. The parameters δ_{p_x}, δ_{p_z}, δ_{m_x} and δ_{m_z} give different types of surface effects. For simplicity, we consider the more common case $\delta > 0$, and a comprehensive discussion was given by Wang and Woo [26]. By separating variables and applying the boundary conditions, the solutions for equations (11) and (12) can be separated into time-dependent and time-independent parts connected by the eigenvalues:

$$\Delta_p(x,z,t) = \mathrm{e}^{\omega_p t}\varphi_{\omega_p}(x,z) = \Delta_0^E \mathrm{e}^{\omega_p t}\cos(k_{px}x)\cos(k_{pz}z), \tag{13}$$

$$\Delta_m(x,z,t) = \mathrm{e}^{\omega_m t}\varphi_{\omega_m}(x,z) = \Delta_0^M \mathrm{e}^{\omega_m t}\cos(k_{mx}x)\cos(k_{mz}z), \tag{14}$$

where ω_p, ω_m are the eigenvalues and φ_{ω_p}, φ_{ω_m} are the corresponding eigenfunctions. According to the stability analysis, the critical conditions are $\omega_p = 0$ and $\omega_m = 0$ for the FE phase and the FM phase, respectively. Thus, the supercooling temperatures are

$$T_c^E = T_{c0}^E - \frac{1}{A^E}(D_{11}^E k_{pz}^2 + D_{44}^E k_{px}^2) + \frac{2}{A^E}\left[(q_{c11} - 2q_{c33}C_{120}/C_{11E})\varepsilon_{11}^0 - f_m q_{c33}/C_{11E}\right], \tag{15}$$

$$T_c^M = T_{c0}^M - \frac{1}{A^M}(D_{11}^M k_{mz}^2 + D_{44}^M k_{mx}^2) + \frac{2}{A^M M_s^2}\lambda_{11}\left[(C_{12}^M - C_{11}^M C_{120}/C_{11M})2\varepsilon_{11}^0 - C_{11}^M f_p/C_{11M} + \frac{1}{3}C_{11}^M(\lambda_{11} - q_{11}^M/C_{11M})\right]. \tag{16}$$

Substituting equations (13) and (14) in the boundary conditions, yields

$$\tan\left(\frac{k_{pz}h}{2}\right) = \frac{1}{k_{pz}\delta_{pz}}, \quad \tan(k_{px}l_p) = \frac{1}{k_{px}\delta_{px}},$$

$$\tan\left(\frac{k_{mz}h}{2}\right) = \frac{1}{k_{mz}\delta_{mz}}, \quad \tan(k_{mz}l_m) = \frac{1}{k_{mx}\delta_{mx}},$$

from which the smallest values of k_{pz}, k_{px}, k_{mz}, k_{mx} can be found. By substituting the results in equations (15) and (16), we obtain the critical temperatures for the phase transitions. The explicit expressions show that the volume fraction and the elastic stresses as well as the length of the element can greatly affect the critical temperatures.

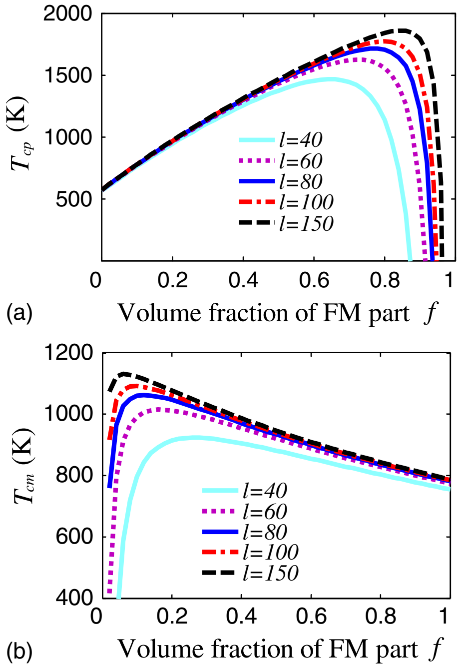

Figure 2. Critical phase transition temperatures versus the volume fraction of the FM phase under different element lengths: (*a*) critical temperature for the FE transition and (*b*) critical temperature for the FM transition.

4. Results and discussions

In this section, we take the BaTiO$_3$–CoFe$_2$O$_4$ system [9] as an example. The material constants (in SI units) are [14, 27]:

$C_{11}^E = C_{22}^E = C_{33}^E = 1.66 \times 10^{11}$,

$C_{12}^E = C_{13}^E = C_{23}^E = 0.77 \times 10^{11}$,

$Q_{11} = Q_{22} = Q_{33} = 0.11$,

$Q_{12} = Q_{13} = Q_{23} = -0.043, \quad A^E = 3.3 \times 10^5$,

$D_{11}^E = 2.7 \times 10^{-9}, \quad D_{44}^E = 0.45 \times 10^{-9}$,

$T_{c0}^E = 383.15; \quad a_p = 3.99, \quad c_p = 4.04, \quad a_m = 8.38/2$,

$c_m = 8.31/2, \quad a_s = 3.905$,

$C_{11}^M = C_{22}^M = C_{33}^M = 2.86 \times 10^{11}$,

$C_{12}^M = C_{13}^M = C_{23}^M = 1.73 \times 10^{11}$,

$\lambda_{100} = -470 \times 10^{-6}$,

$M_s = 4.66 \times 10^3, \quad \chi = 4.7 \times 10^3, \quad T_{c0}^M = 793$

$D_{11}^M = 7.2 \times 10^{-17}, \quad D_{44}^M = 3.6 \times 10^{-17}$.

Because of the limitations of the experimental data, D_{11}^M and D_{44}^M are given with considerable values, but the approximation should be sufficient for our discussion. The values for the extrapolation lengths are usually about 5–45 nm for BaTiO$_3$; here, 45 nm is used for both the phases. The thickness of the film is set to be 200 nm and the element length l is set to be adjustable to probe the length effect.

In fact, the dislocations also have a great effect on the thin film [28] and here we just give a cut of the stress values induced by the lattice mismatch, namely ε_{11}^0 $(= \varepsilon_{22}^0)$ is multiplied by a factor of 0.1 to be closer to the experiment. Figure 2 shows the critical temperatures versus the volume fraction under different element lengths l. Obviously, by considering T_{cp} and T_{cm} to be valid (above 0 K), there are minimal sizes corresponding to the different volume fractions. The rapid decreases in T_{cp} and T_{cm} are regarded as the size effects, which are common phenomena

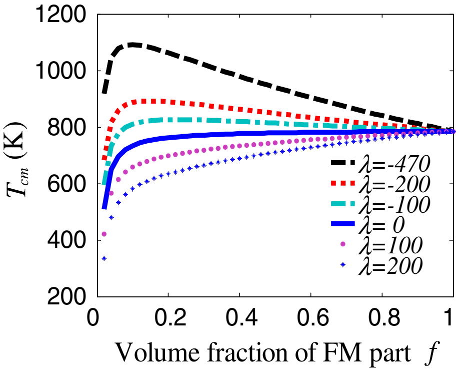

Figure 3. Critical magnetic phase transition temperatures versus the volume fraction of the FM phase under different magnetostrictive values $\lambda(\times 10^{-6})$ ($l = 100$ nm).

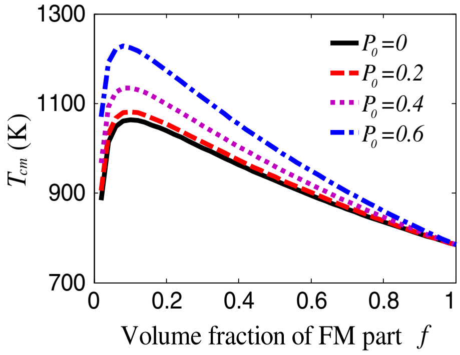

Figure 4. Critical magnetic phase transition temperatures versus the volume fraction of the FM phase under different polarization values ($l = 100$ nm, P_0 is in C m^{-2}).

in the FE and the FM materials. As shown in figure 2(*a*), within the valid value, the critical transition temperature for the FE phase shows a notable increase with a maximum value about 4 times higher than that of the bulk and the corresponding value of f is more than 0.5 increasing towards longer l. It is properly due to the larger lattice mismatch with a bigger volume fraction of $CoFe_2O_4$ whose lattice parameters deviate more from those of the substrate. The case in the FM phase (figure 2(*b*)) is rather different. Except for the sharp rise for the small value of f due to the size effect, a slight decrease is manifested with the increase in f. Because of the small value of the magnetostrictive coefficients, the contribution of the stress is small to T_{cm}, as illustrated in equation (16). In fact, there are two cases of the stress effect on the two phases. One is that the compressive stress arising from the lattice mismatch of the substrate and the thin film is big enough to make both of the phases elongating along the z axis, which redounds to the FE phase transition while hampering the FM phase transition because of the negative value of the magnetostrictive coefficient; the other is that the substrate compression is proper to make the lattice of the FM phase depresses along the z axis while extends in the FE phase. Such a balance favours a transition in both the FE and the FM phases and results in lower critical temperatures. The situation will be different in a system with a positive magnetostrictive material or different directions of easy axes, adding complexities to the design of two-phase multiferroic materials with a large ME effect. To probe more details about the effect of the λ value, we studied T_{cp} and T_{cm} versus the volume fraction f under different values of λ. The results shown in figure 3 reveal that T_{cm} is higher with the negative values than the positive ones and reaches a maximum when f is about 0.3. Because of the small magnetostrictive value, the effect of magnetostrictive stress on T_{cp} is insignificant. In particular, the FM phase transition temperature also changes significantly with the value of P as given in figure 4, while the value of M does not affect the FE transition temperature.

5. Summary and conclusions

By using a bifurcation analysis, a thermodynamic model for investigating the critical temperatures of the FE and the FM transitions for the epitaxial 1–3 type multiferroic thin films are established. Our results show that the properties of the phase transitions are greatly affected by the induced stresses and can be controlled by adjusting the volume fraction of the FM phase within the film. The critical temperature of the phase transition in the FM phase changes significantly with the characters of the FE phase, but was not the same with the FE phase because of the small magnetostrictive value. Analytic expressions also show that the misfit stresses induced by the lattice mismatch are crucial in determining the transition temperatures of the multiferroic materials.

Acknowledgments

This project was supported by the National Science Foundation of China (Nos 50232030, 10172030 and 10572155) and the Science Foundation of Guangdong Province (2005A10602002).

References

[1] Fiebig M, Lottermoser Th, Fröhlich D, Goltsev A V and Pisarev R V 2002 *Nature* **419** 818
[2] Hill N A 2000 *J. Phys. Chem.* B **104** 6694
[3] Son J Y, Kim B G, Kim C H and Cho J H 2004 *Appl. Phys. Lett.* **84** 4971
[4] Wang J *et al* 2003 *Science* **299** 1719
[5] Pio B, Claude E and Nicola A S 2005 *Phys. Rev.* B **72** 214105
[6] Kimura T, Goto T, Shintani H, Ishizaka K, Arima T and ToKura Y 2003 *Nature* **426** 55
[7] Hur N, Park S, Sharma P A, Ahn J S, Guha S and Cheong S W 2004 *Nature* **429** 392
[8] Srinivasan G, Rasmussen E T, Levin B J and Hayes R 2002 *Phys. Rev.* B **65** 134402
[9] Zheng H *et al* 2004 *Science* **303** 661
[10] Nan C W, Liu L, Cai N, Zhai J, Ye Y, Lin Y H, Dong L J and Xiong C X 2002 *Appl. Phys. Lett.* **81** 3831
[11] Schtelen J van 1972 *Philips Res. Rep.* **27** 28
[12] Lin Y H, Cai N, Zhai J Y, Liu G and Nan C W 2005 *Phys. Rev.* B **72** 012405
[13] Zhai J, Dong S, Xing Z, Li J and Viehland D 2006 *Appl. Phys. Lett.* **89** 083507
[14] Eerenstein W, Mathur N D and Scott J F 2006 *Nature* **442** 759
[15] Nan C W, Liu G, Lin Y H and Chen H 2005 *Phys. Rev. Lett.* **94** 197203
[16] Liu G, Nan C W, Xu Z K and Chen H 2005 *J. Phys. D: Appl. Phys.* **38** 2321
[17] Zavaliche F *et al* 2005 *Nano Lett.* **5** 1793–6

[18] Li Y L, Hu S Y, Liu Z K, Chen L Q 2002 *Acta Mater.* **50** 395–411

[19] Duan C G, Jaswal S S and Tsymbal E Y 2006 *Phys. Rev. Lett.* **97** 047201

[20] Chambers S A, Farrow R F C, Maat S, Toney M F, Folks L, Catalano J G, Trainor T P and Brown G E 2002 *J. Magn. Magn. Mater.* **246** 124

[21] Rijnders G and Blank D H A 2005 *Nature* **433** 369

[22] Toshio M 1987 *Micromechanics of Defects in Solids* 2nd edn (London: Martinus Nijhoff) p 5

[23] Alex H and Rudolf S 2000 *Magnetic Domains: The Analysis of Magnetic Microstructures* (Berlin: Springer) p 136

[24] Wang B and Woo C H 2004 *Acta Mater.* **52** 5639

[25] Amikam A 2000 *Introduction to the Theory of Ferromagnetism* 2nd edn (Oxford: Oxford University Press) p 63

[26] Wang B and Woo C H 2005 *J. Appl. Phys.* **97** 084109

[27] Waldron R D 1955 *Phys. Rev.* **99** 1727

[28] Zheng Y, Wang B and Woo C H 2006 *Appl. Phys. Lett.* **88** 092903